



Carbon supported Ru-Ni bimetallic catalysts for the enhanced one-pot conversion of cellulose to sorbitol



Lucília S. Ribeiro^a, Juan J. Delgado^b, José J.M. Órfão^a, M. Fernando R. Pereira^{a,*}

^a Laboratório de Processos de Separação e Reação – Laboratório de Catálise e Materiais (LSRE-LCM), Departamento de Engenharia Química, Faculdade de Engenharia, Universidade do Porto, Rua Dr. Roberto Frias, 4200-465 Porto, Portugal

^b Departamento de Ciencia de los Materiales e Ingeniería Metalúrgica y Química Inorgánica, Facultad de Ciencias, Universidad de Cádiz, Campus Rio San Pedro, 11510 Puerto Real, Cádiz, Spain

ARTICLE INFO

Article history:

Received 18 January 2017

Received in revised form 30 March 2017

Accepted 5 April 2017

Available online 1 June 2017

Keywords:

Cellulose

Sorbitol

Hydrolytic hydrogenation

Ru-Ni catalysts

ABSTRACT

Ru and Ni mono- and bimetallic catalysts were prepared by impregnation of two different supports (activated carbon and carbon nanotubes) and were characterized by TPR, TEM and N₂ adsorption at –196 °C. The prepared Ru mono- and bimetallic catalysts were highly efficient for the hydrolytic hydrogenation of cellulose to sorbitol. Regardless of the support used, when nickel was incorporated into the supported ruthenium catalyst a promoting effect was observed, with an increase in both conversion and selectivity to sorbitol, which was explained by the interaction between both metals. Yields of sorbitol around 50–60% were achieved after 5 h of reaction when using Ru-Ni/AC and Ru-Ni/CNT as catalysts. Moreover, a yield of sorbitol over 70% could be reached in just 1 h of reaction if the Ru-Ni catalysts were ball-milled together with cellulose.

© 2017 Elsevier B.V. All rights reserved.

1. Introduction

Currently, the use of renewable feedstocks for chemicals, fuels and energy has achieved an increasing attention due to the depletion of fossil fuels and the problems arising from global warming [1–3]. Lignocellulosic biomass is considered a promising alternative source to fossil fuels for the sustainable production of fuels and chemicals [4,5]. Cellulose is the most abundant form of biomass and its hydrolytic hydrogenation into sugar alcohols (such as sorbitol) is gaining increasing interest as an attractive alternative in its valorisation [6,7]. Sorbitol has been identified as one of the twelve most important building blocks derived from biomass resources [8] as can be used in food industry, pharmaceuticals, cosmetics, textiles and industrial applications, or as reactant in processes that yield other high added-value products [9]. The conversion of cellulose into sugar alcohols consists of two consecutive steps: hydrolysis of cellulose to glucose via cellooligosaccharides [10–12] and hydrogenation of glucose to sugar alcohols over metals [13,14]. Recently, it was shown that cellulose can be directly converted into sugar alcohols by the use of heterogeneous catalysts [15–17], instead of

the traditional use of liquid acids required to perform the hydrolysis of cellulose to glucose [18].

In 2006, Fukuoka and Dhepe reported the first hydrolytic hydrogenation of cellulose using only solid catalysts and obtained a yield of sorbitol of 25% using Pt/γ-Al₂O₃ [19]. Being known as heat- and water-tolerant supports, carbons such as activated carbon (AC) and carbon nanotubes (CNT) have been extensively studied as catalyst supports in the conversion of cellulose [20]. Luo et al. reported 30% yield of sorbitol using Ru/AC [21] and Deng et al. attained 69% using Ru/CNT and H₃PO₄ pre-treated cellulose [22]. Geboers et al. obtained a yield of sugar alcohols of 85% from ball-milled cellulose by the mixture of Ru/AC and heteropoly acid H₄SiW₁₂O₄₀ [23]. Though this is one of the best sugar alcohols yield ever attained, it involved the use of acids, thus being a non-environmentally friendly approach. Kobayashi et al. presented an innovative method for an efficient hydrolysis of cellulose to glucose by ball-milling the cellulose together with the catalyst [10], denoted as mix-milling, and then the method was also applied for the hydrolytic hydrogenation of cellulose by Komanoya et al. using a ruthenium catalyst [24]. Later, we also reported a yield of sorbitol of 69% by mix-milling Ru/AC with cellulose as pre-treatment, without the use of any acids [25]. More recently, Ni catalysts have been also studied [20,26]. Microcrystalline cellulose was converted to sorbitol over Ni₂P/AC [27] and Ni₁₂P₅/AC [28] with yields of 48 and 62%, respectively, but these catalysts showed to be not durable in hot water due to phosphorous leaching and Ni sintering. In contrast, Ni sup-

* Corresponding author.

E-mail addresses: lucilia@fe.up.pt (L.S. Ribeiro), juan jose.delgado@uca.es (J.J. Delgado), jjmo@fe.up.pt (J.J.M. Órfão), fpereira@fe.up.pt (M.F.R. Pereira).

ported on carbon nanofibers (CNF) was stable for 24 h at 210 °C and gave sorbitol (64%) with 93% conversion of cellulose [29]. Bimetallic catalysts containing Ni have also shown to be effective for the hydrolytic hydrogenation of cellulose to sorbitol and a 58% yield of sugar alcohols was attained using Ir-Ni supported on mesoporous carbon (MC) [30].

An optimization of the catalyst can be done by the combination of active sites (metals), supports and promoters. Bimetallic catalysts are showing up as a promising option since the interaction between metals can modify the properties of the catalyst, which can result in an improvement of the catalytic activity, modification of the selectivity to the desired product and increase in the catalyst stability [31–34]. Accordingly, new bimetallic catalysts need to be optimized ensuring high reaction rates and high selectivities to the desired products. Herein, we report an efficient one-pot conversion of cellulose to sorbitol using Ru-Ni catalysts supported on activated carbon and carbon nanotubes.

2. Materials and methods

2.1. Chemicals and materials

Microcrystalline cellulose, activated carbon GAC 1240 PLUS and Nanocyl-3100 multi-walled carbon nanotubes were provided by Alfa Aesar, Norit and Nanocyl, respectively. The metal precursors ruthenium (III) chloride (RuCl_3 99.9%, Ru 38% min) and nickel (II) nitrate hexahydrate ($\text{Ni}(\text{NO}_3)_2 \cdot 6\text{H}_2\text{O}$, 99.999%) were supplied by Alfa Aesar and Sigma-Aldrich, respectively. Sulphuric acid was purchased from VWR. All solutions were prepared in ultrapure water obtained in a Milli-Q Millipore System with a conductivity of $18.2 \mu\text{S cm}^{-1}$.

2.2. Preparation of materials

Microcrystalline cellulose was ball-milled in a ceramic pot with two ZrO_2 balls using a laboratory equipment (Retsch Mixer Mill MM200), operating at a frequency of 20 Hz for 4 h (see details in [25]).

Two 0.4% wt. ruthenium catalysts and two 3% wt. nickel catalysts were prepared via incipient wetness impregnation of an aqueous solution of the corresponding precursor on activated carbon (AC, sieved between 100 and 300 μm) and carbon nanotubes (CNT). The resulting materials were dried overnight at 110 °C. Next, the catalysts were submitted to heat treatment under a N_2 flow of $50 \text{ cm}^3 \text{ min}^{-1}$ for 3 h and reduction under H_2 flow of $50 \text{ cm}^3 \text{ min}^{-1}$ for 3 h. The appropriate reduction temperatures (250 °C for Ru catalysts and 500 °C for Ni catalysts) were determined by temperature programmed reduction (TPR) analyses (see Section 3.1). The heat treatment was carried out at the same temperature used for the reduction. The samples were denoted as Ru/AC, Ru/CNT, Ni/AC and Ni/CNT.

Two 0.4%Ru-3%Ni bimetallic catalysts were prepared via incipient wetness impregnation of an aqueous solution of RuCl_3 on the already prepared Ni/AC and Ni/CNT catalysts (heat treated and reduced at 500 °C). After impregnation, the samples were dried overnight at 110 °C. Next, they were treated under a N_2 flow of $50 \text{ cm}^3 \text{ min}^{-1}$ for 3 h at 250 °C and reduced under H_2 flow of $50 \text{ cm}^3 \text{ min}^{-1}$ for 3 h at 250 °C. The samples were denoted as Ru-Ni/AC and Ru-Ni/CNT.

In order to evaluate the effect of the Ni incorporation method, besides preparing the Ru-Ni/CNT catalyst sequentially as described above, the Ru-Ni catalyst was also prepared via incipient wetness co-impregnation of an aqueous solution of both precursors (RuCl_3 and $\text{Ni}(\text{NO}_3)_2 \cdot 6\text{H}_2\text{O}$) on the support (CNT). After this, the catalyst was dried overnight at 110 °C and then submitted to heat treatment

under a N_2 flow of $50 \text{ cm}^3 \text{ min}^{-1}$ for 3 h at 500 °C and reduction under H_2 flow of $50 \text{ cm}^3 \text{ min}^{-1}$ for 3 h at 500 °C. This sample was denoted as Ru-Ni/CNT_500.

Since in this last prepared bimetallic catalyst the Ru was treated and reduced at 500 °C, for comparative purposes another ruthenium catalyst (0.4% wt.) was prepared on CNT according to the same procedure as the other monometallic catalyst, but it was heat treated and reduced at 500 °C. This catalyst was denoted as Ru/CNT_500.

2.3. Characterization of materials

The temperatures of the activation steps (heat treatment and reduction) required to ensure the complete reduction of ruthenium and nickel precursors were determined by TPR, using a fully automated AMI-200 equipment (Altamira Instruments).

The supports and catalysts were characterized by N_2 adsorption at -196°C using a Quantachrome NOVA Surface Area and Pore Size analyser. Surface area calculations were made using the Brunauer-Emmett-Teller (BET) equation, and the micropore volumes (V_{micro}) and mesopore surface areas (S_{meso}) were determined by the t -method. Further details can be found elsewhere [25].

The surface morphology and metal particle size distribution of the mono- and bimetallic catalysts were analysed by transmission electron microscopy (TEM) using a JEOL2010F instrument equipped with an Oxford X-Max^N 80 T X-ray energy dispersive spectrometer. High Angle Annular Dark Field-Scanning Transmission Electron Microscopy (HAADF-STEM) images were obtained with the same microscope using a 0.5 nm probe and a camera length of 10 cm. This mode allows to control the position of the electron beam (0.5 nm) and obtain the XEDS analysis of the irradiated area. Size distributions were determined by the measurement of at least 200 random particles and the average diameter was calculated by $d_M = \frac{\sum d_i n_i}{\sum n_i}$, where n_i is the number of particles with diameter d_i . Metal dispersion was obtained using the following equation: $D = \frac{\sum N_{\text{Si}}}{\sum N_{\text{Ti}}}$, where N_{Si} and N_{Ti} correspond to the number of atoms on the surface and the total amount of atoms of each particle, respectively. Gauss software, Rhodius and Eje Z software were used to create a model of the nanoparticles and determine the total amount of atoms of each particle and those located at the surface [35,36].

2.4. Catalyst evaluation

The catalytic experiments were performed in a 1000 mL stainless steel Parr reactor. In a typical experiment, ball-milled cellulose (750 mg) and catalyst (300 mg) were added to 300 mL of water and loaded in the autoclave, which was then flushed three times with nitrogen to remove the ambient air. Subsequently, the mixture was heated to 205 °C and stirred at 150 rpm. When the desired temperature was achieved, the system was pressurized with hydrogen (50 bar). The reaction was stopped after 5 h and the pH was measured at the beginning and end of the reaction. The catalyst was separated by centrifugation and filtration.

The reaction liquid mixtures were analysed by high performance liquid chromatography (HPLC) using an Alltech OA-1000 ion exclusion column and a refractive index (RI) detector. A 0.005 mol L^{-1} H_2SO_4 mobile phase was used as the eluent with a 0.5 mL min^{-1} flow rate. An injection volume of 30 μL and a measuring time of 20 min were selected. Sorbitol, mannitol, glucose, erythritol, glycerol, ethylene glycol (EG) and propylene glycol (PG) were the products detected. The yield of each product was defined as the number of moles of product formed divided by the total number of moles of cellulose initially present, taking the stoichiometry into consideration; the selectivity was defined as the ratio between the

Table 1
Textural properties of the different materials.

Sample	S_{BET} ($\text{m}^2 \text{g}^{-1}$)	S_{meso} ($\text{m}^2 \text{g}^{-1}$)	V_{micro} ($\text{cm}^3 \text{g}^{-1}$)
AC	847	145	0.301
Ru/AC	804	152	0.294
Ni/AC	763	144	0.276
Ru-Ni/AC	807	182	0.275
CNT	267	267	–
Ru/CNT	265	265	–
Ru/CNT.500	266	266	–
Ni/CNT	239	239	–
Ru-Ni/CNT	256	256	–
Ru-Ni/CNT.500	261	261	–

yield of each product and the conversion of cellulose. For determining the conversion of cellulose, total organic carbon (TOC) data was obtained with a Shimadzu TOC 5000-A and the conversion was calculated as the ratio of the number of moles of TOC in the resultant liquid to the number of moles of carbon in the cellulose initially charged to the reactor. Typical selectivities absolute error in the catalytic experiments was within $\pm 3\%$.

3. Results and discussion

3.1. Characterization of materials

The reducibility of the prepared catalysts was studied by TPR. The profiles of the mono- and bimetallic Ru-Ni samples are displayed in Fig. 1. It can be noticed that the monometallic Ru samples present a reduction peak with a maximum at lower temperature than the monometallic Ni samples. Activated carbon supported ruthenium and nickel monometallic catalysts show wide reduction peaks around 100–300 °C and 250–450 °C, respectively (Fig. 1a), while carbon nanotubes supported Ru and Ni monometallic catalysts present reduction peaks around 150–350 °C and 200–350 °C, respectively (Fig. 1b). For all the Ru-Ni catalysts, the reduction occurs around 300 °C, which is between the reduction temperatures of the respective monometallic Ru and Ni catalysts, and so it can be assigned to the promoted reduction of Ni oxides originated by the presence of Ru. The decrease in the reduction temperature of activated carbon supported nickel in bimetallic catalysts induced by the presence of ruthenium clearly indicates that an intimate contact between nickel and ruthenium species was achieved. In the case of carbon nanotube supported catalysts, the TPR profile of Ru-Ni/CNT shows that the reduction peak maximum shifted slightly to lower temperatures comparatively to Ni monometallic catalyst, again suggesting that the presence of ruthenium facilitates the reduction of nickel due to an interaction between both elements. According to these results, and for comparative purposes, to assure effective reduction of the metal and also to minimize its sintering, reduction temperatures of 250 °C and 500 °C were selected for ruthenium and nickel, respectively.

Table 1 summarizes the textural properties of the supports and catalysts determined from N_2 adsorption at -196°C . Carbon nanotubes present a surface area of $267 \text{ m}^2 \text{g}^{-1}$ and an adsorption isotherm of type II, which is typical of non-microporous materials. On contrary, activated carbon presents a much higher BET surface area ($847 \text{ m}^2 \text{g}^{-1}$) according to their well-developed microporosity. Whereas AC has a considerable amount of micropores ($0.301 \text{ cm}^3 \text{g}^{-1}$), most of the porosity observed in CNT corresponds to large mesopores, which result from the free space in carbon nanotube bundles. In fact, CNT are not used individually but as aggregates leading to the formation of pores.

As expected, no major differences in the textural properties of the materials were observed, since only a slight decrease in the BET surface area and micropores volume was noticed with the introduc-

Table 2
Average crystallite size (d_M) and metal dispersion (D) of the different catalysts.

Catalyst	d_M (nm)		D (%)	
	Ru	Ni	Ru	Ni
Ru/AC	1.4 ± 0.1	–	66	–
Ni/AC	–	8.8 ± 0.6	–	11
Ru-Ni/AC	1.5 ± 0.2	9.9 ± 0.7	57	5
Ru/CNT	1.0 ± 0.1	–	74	–
Ru/CNT.500	1.9 ± 0.2	–	44	–
Ni/CNT	–	9.7 ± 0.7	–	9
Ru-Ni/CNT	1.7 ± 0.2	4.5 ± 0.4	50	13
Ru-Ni/CNT.500	1.9 ± 0.2	9.5 ± 0.6	42	5

tion of the metallic phases. These decreases were more pronounced upon the introduction of the Ni phase since its metal loading (3%) is higher than the loading of Ru (0.4%).

HAADF images and metal particle size distributions of the mono- and bimetallic supported catalysts are presented in Figs. 2–4. The characterization by this technique, which is sensitive to the atomic number, in combination with XEDS analysis demonstrates that the nanoparticles smaller than 4 nm in the Ru-Ni catalysts correspond to monometallic Ru nanoparticles or with a high concentration of Ru (>75% weight) (Fig. 4). On the other hand, the metal nanoparticles bigger than 5 nm exhibited Ni contents higher than 95%. No formation of a Ru-Ni alloy was observed for any catalyst, but a close proximity between metals. For example, for the Ru-Ni/AC catalyst, Ni particles with several small Ru particles on its surface could be observed (Fig. 5), and this intimate contact at nano-level between the Ru and Ni particles would justify the decrease in the reduction temperature of nickel oxide in Ru-Ni/AC, induced by the presence of Ru, as discussed above. On the other hand, TEM results show that these Ni particles with Ru on the surface were much less frequent on CNT supported Ru-Ni catalysts, which explains why only a slight shifting of the reduction peak was observed for Ru-Ni/CNT comparatively to Ni/CNT (see Fig. 1). However, in Ru-Ni/CNT.500 isolated Ru and Ni particles are observed (Fig. 4c). Table 2 shows the average Ru and Ni particle sizes, as well as dispersions. A good dispersion of Ru nanoparticles can be noticed on both supports (Fig. 2 and Table 2). The average size of the ruthenium particles in the prepared catalysts ranges from 1.0 to 1.9 nm with metal dispersions from 42 to 74% (Table 2). A counting of ruthenium and nickel particles from HAADF images was performed. Histograms in Figs. 3 and 4 present metal particle size distributions for the prepared mono- and bimetallic catalysts, respectively. As can be observed, the Ni particles present much higher average particle diameters and a much lower metal dispersion compared to the Ru particles. The average size of the nickel particles in Ni/AC and Ni/CNT is 8.8 and 9.7 nm and the metal dispersions are 11 and 9%, respectively (Table 2). The particle size distribution of each metal does not vary significantly with the support (Fig. 3).

From the results obtained in Table 2, it can be observed that reduction at higher temperatures originates a decrease in the ruthenium dispersion from 74 to 44% and from 50 to 42% for mono- and bimetallic catalysts, respectively, which can be attributed to an increase in the metallic particle sizes (see Figs. 3 and 4) due to sintering during the heat treatment and reduction steps. The decrease in the metallic dispersion caused by particle agglomeration after reduction at 500 °C was much smaller in Ru-Ni/CNT.500 than in Ru/CNT.500, indicating a better stability against sintering in the former case.

The ball-milling of microcrystalline cellulose originated a great decrease in its crystallinity degree, which was initially 92% (Fig. S1). The ball-milled cellulose used in this work had a crystallinity of 23% and a degree of polymerization of 192, as determined by X-ray powder diffraction and by the viscosity method, respectively.

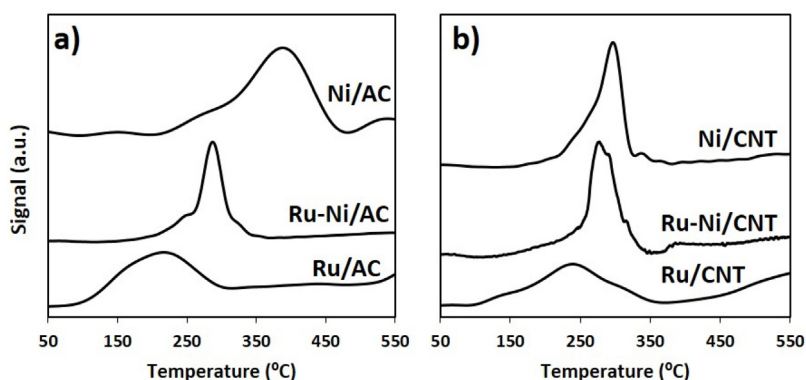


Fig. 1. TPR profiles of a) activated carbon and b) carbon nanotubes supported catalysts.

Details for the characterization of cellulose can be found elsewhere [25].

3.2. Catalytic conversion of cellulose

First, a blank test (without catalyst) was carried out. A conversion of cellulose of 20% and a yield of sorbitol of 7% were achieved after 5 h of reaction. Experiments with the supports (without metal phases) were also performed. In these experiments, 750 mg of ball-milled cellulose and 300 mg of support (AC or CNT) were loaded into the reactor under the reaction conditions described in the experimental section (Section 2.4), and a yield of sorbitol around 8% was obtained for both supports, with cellulose conversions up to 25%, indicating that the metal is required to achieve a selective conversion of cellulose to sorbitol. The influence of the reaction temperature was firstly studied and the results indicated a maximum of polyols selectivity at 205 °C, since it started to decrease at higher temperatures, due to the formation of undesirable by-products. So, considering energy consumption, cellulose conversion and the selectivity to polyols (especially sorbitol), the temperature selected for performing the standard tests was 205 °C. The influence of the initial concentration of cellulose on its direct conversion to sorbitol was not presented, since in a previous work [37] we had already studied this effect by varying the amount of cellulose (ball-milled at 10 Hz for 4 h) loaded to the reactor from 300 to 3000 mg. Since the conversions obtained were practically the same and the selectivity to sorbitol reached a maximum for 750 mg, we have selected this amount for the present study.

Four monometallic catalysts (Ru/AC, Ni/AC, Ru/CNT and Ni/CNT) were then tested in the one-pot hydrolytic hydrogenation of cellulose. Although the conversion did not vary significantly (Table 3), the results show that the Ru catalysts are much more selective to sorbitol than Ni catalysts (Table 3 and Fig. 6), which could be related to the great difference observed between the average particle size and dispersion of each metal (Ru and Ni) on the support (Table 2) and mainly to the nature of the metal. An increase of 35% and 43% in the yield of sorbitol after 5 h was observed when using Ru/AC instead of Ni/AC (Fig. 6a) and Ru/CNT instead of Ni/CNT (Fig. 6b), respectively. Fig. 6 also shows that the Ni monometallic catalysts greatly favour the formation of other secondary products (not analysed in this work), with selectivities up to 67% after 5 h for both catalysts (Ni/AC and Ni/CNT). The results indicate that the Ru atoms are the active sites for the direct production of sorbitol from cellulose. Besides the main product (sorbitol), other products as glucose, erythritol, glycerol, mannitol, ethylene glycol (EG) and propylene glycol (PG) were also detected for these catalysts, but none of them exceeds 13% in selectivity (Table 3). The pH of the medium changed from around 7 to 4 from the beginning to the end of the experiments (5 h), indicating that acid by-products are formed as the reaction

progresses. Furthermore, Ru/CNT showed to be more selective to sorbitol than Ru/AC, which can be explained by the better dispersion of ruthenium on CNT (74%) comparatively to AC (66%) (Table 2) and/or by the different textural properties of the two supports, indicating that a mesoporous material could be more efficient as catalytic support for the direct conversion of cellulose to sorbitol. Pang et al. have also reported that mesoporous carbon supported catalysts are much more efficient than the AC supported counterpart for the conversion of cellulose [30], and concluded that the different performances were mainly originated from the different nature of the carbon materials used as supports.

Two Ru-Ni catalysts (Ru-Ni/AC and Ru-Ni/CNT) were also studied for this reaction (Fig. 6). Different Ru-Ni ratios were previously studied by varying the Ni loading from 1 to 5 wt.% and maintaining the Ru loading (0.4 wt.%), and the 0.4Ru-3%Ni catalysts showed to be the most selective to sorbitol (Figs. S2 and S3). Accordingly, this ratio was selected for the catalytic studies. The conversion of cellulose after 5 h of reaction remained practically unchanged when using Ru-Ni/AC comparatively to Ru/AC (Table 3). On the opposite, when using Ru-Ni/CNT, the conversion of cellulose after 5 h increased from 83.5 to 99.7%, when compared to the respective Ru monometallic catalyst (Table 3). Pang et al. had already tested Ru-Ni bimetallic catalysts supported on mesoporous carbon and observed an increased conversion of cellulose by the addition of Ru to the Ni monometallic catalyst (from 84.5 to 100%) [30], which is in accordance to the results obtained here. In addition, carbon nanotube supported mono- and bimetallic catalysts presented conversions of cellulose around 84–100% after 5 h of reaction, which were higher than those observed using the activated carbon supported catalysts (conversions around 78–88%). In terms of product distributions, Ru/CNT and Ru-Ni/CNT also showed to be more selective to sorbitol after 5 h of reaction than Ru/AC and Ru-Ni/AC. As for the Ru-Ni catalysts, it is quite clear that, besides the conversion of cellulose, the yield of sorbitol could also be increased with the addition of Ni to the Ru catalysts (Fig. 6). In this case, selectivities to sorbitol around 60% were attained after 5 h of reaction for both bimetallic catalysts. It should be highlighted that such selectivities to sorbitol could be achieved after just 1 h of reaction when using the Ru-Ni catalyst(s). Moreover, the results indicate that apparently there is a synergetic effect between ruthenium and nickel, being the former the catalytically active and selective specie in the direct conversion of cellulose to sorbitol since nickel monometallic catalysts presented sorbitol selectivities not higher than 8%, in the same order of the blank test. This synergetic effect is not due to the formation of a Ru-Ni alloy, but results from a close proximity of Ru and Ni, as already discussed in Section 3.1. Table 3 also shows the evolution of the selectivity to sorbitol from 1 to 5 h of reaction. Regardless of the support used, for the Ru mono- and bimetallic catalysts an increase of the selectivity

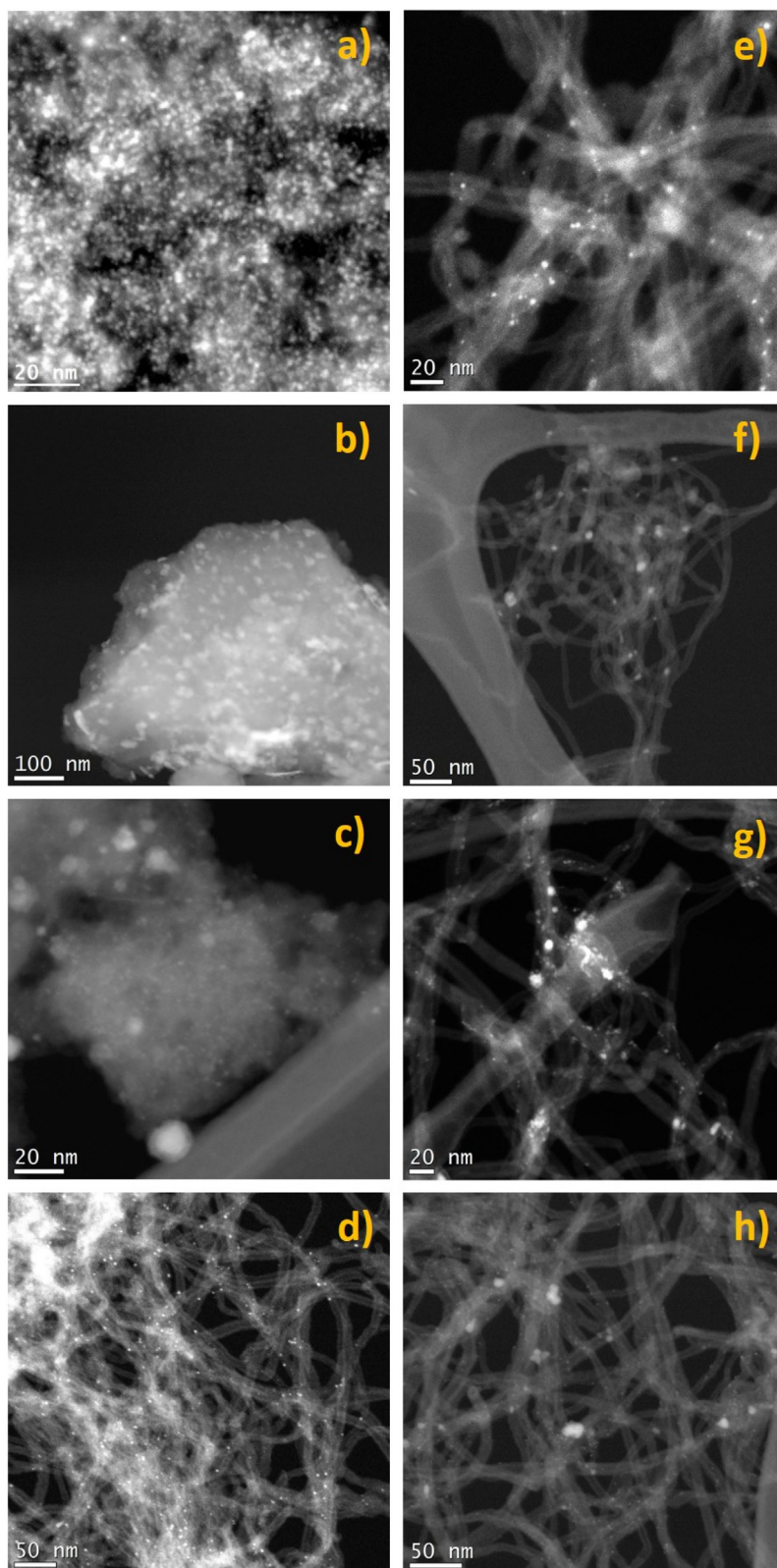


Fig. 2. TEM micrographs of the catalysts: a) Ru/AC, b) Ni/AC, c) Ru-Ni/AC, d) Ru/CNT_500, e) Ru/CNT, f) Ni/CNT, g) Ru-Ni/CNT, and h) Ru-Ni/CNT_500.

to sorbitol with time is evident, on contrary to what occurs with the Ni monometallic catalysts.

In order to determine whether the intimate contact between Ru and Ni was responsible for the improved performance of the bimetallic catalysts, the Ru and Ni monometallic catalysts were

mixed mechanically and then tested for the conversion of cellulose under the same conditions and the results are included in Fig. 6 and Table 3. When using AC as support, no significant differences could be observed on the conversion of cellulose and sorbitol yield over the mixed Ru/AC and Ni/AC catalysts when compared to the

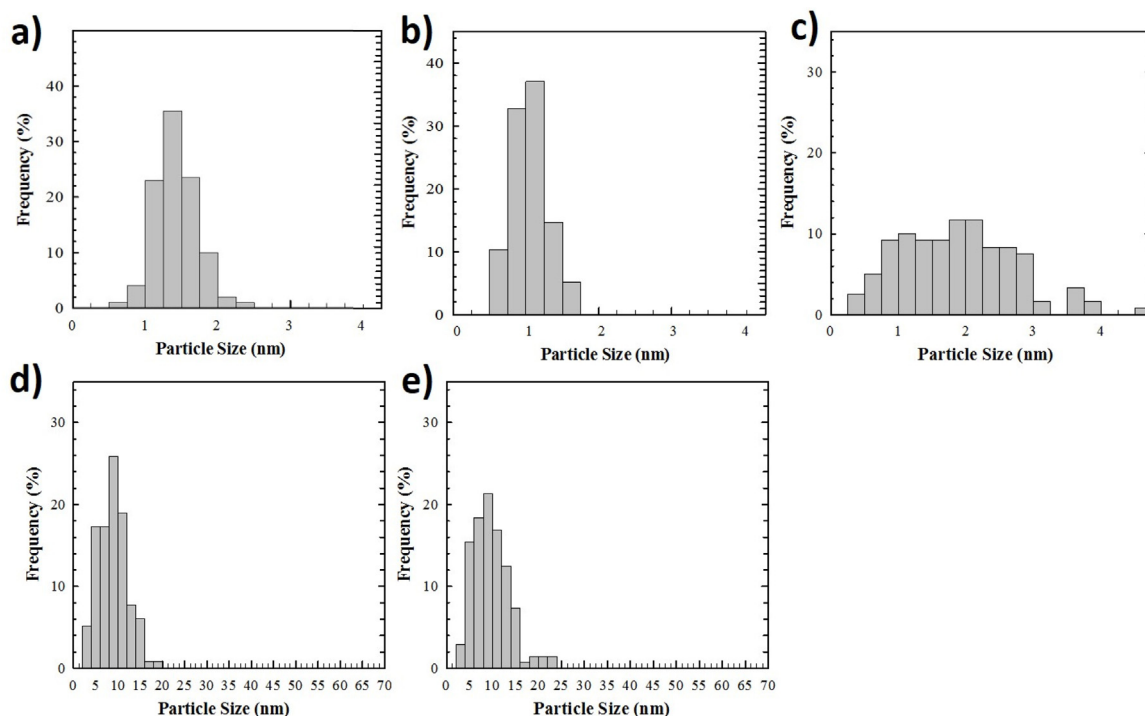


Fig. 3. Metal particle size distribution of the monometallic catalysts: a) Ru/AC, b) Ru/CNT, c) Ru/CNT.500, d) Ni/AC, and e) Ni/CNT.

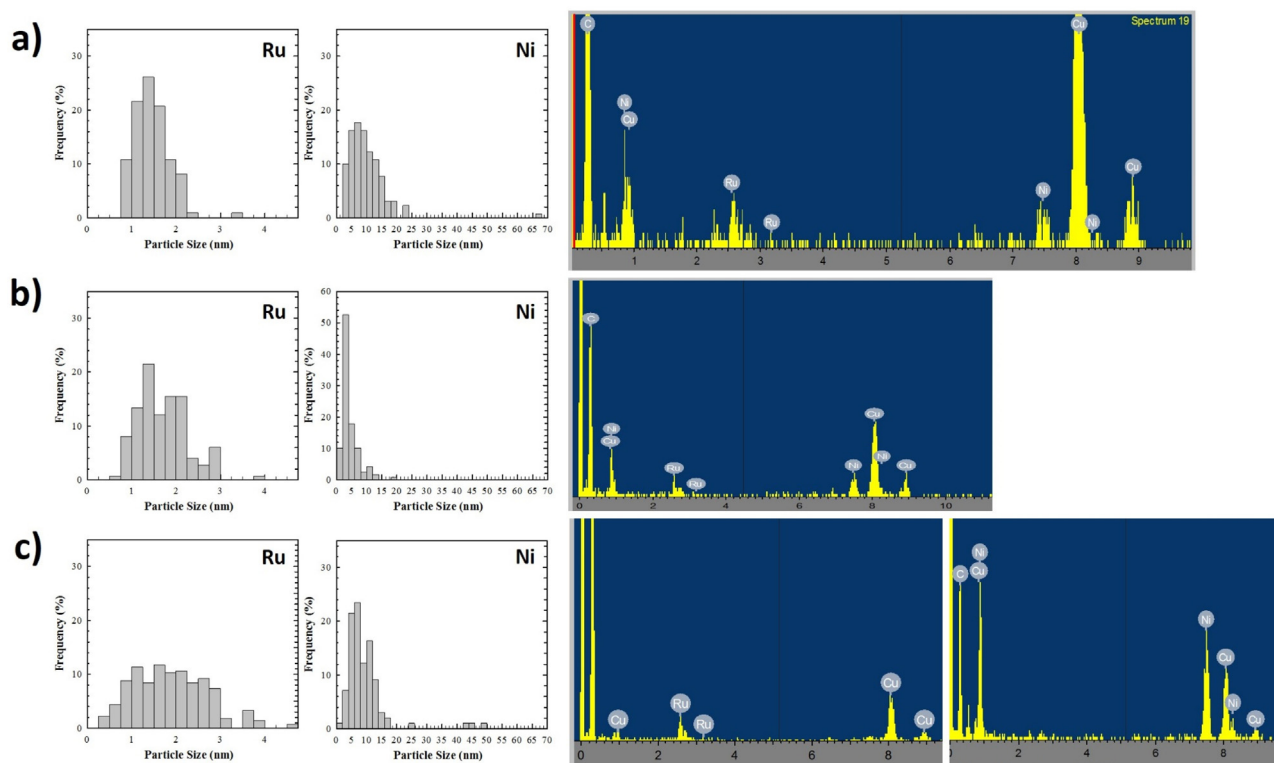


Fig. 4. Metal particle size distributions and XEDS analysis of the Ru-Ni catalysts: a) Ru-Ni/AC, b) Ru-Ni/CNT, and c) Ru-Ni/CNT.500.

individual Ru/AC catalyst (Table 3). However, comparatively to the individual Ru/CNT catalyst, the mixed Ru/CNT and Ni/CNT catalysts presented a decrease in the conversion of cellulose after 1 h of reaction, as well as in the selectivity to sorbitol after 1 and 5 h of reaction (Table 3). Although many reactions can be involved in the process of converting cellulose into sorbitol, sequentially taking

place on different types of catalytic sites and proceeding independently, these results strongly suggest that the synergetic effect observed between Ru and Ni requires a close proximity between the two metallic components, but not necessarily in contact with each other, and that it is not sufficient that both metals are present in the reaction system.

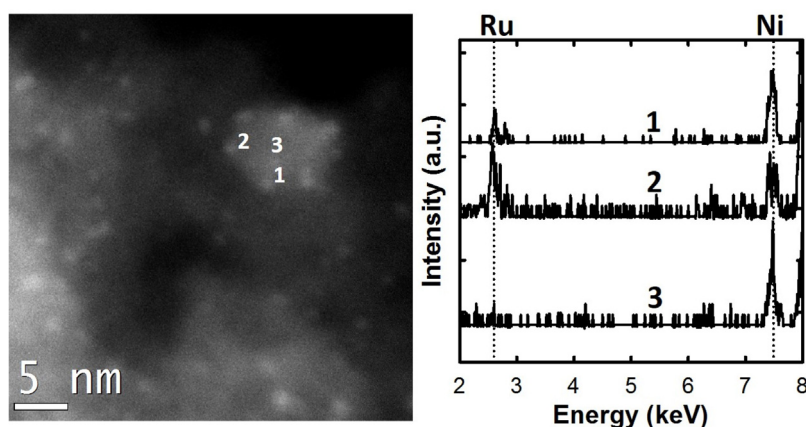


Fig. 5. TEM micrograph and XEDS analysis of the Ru-Ni/AC catalyst.

Table 3

Comparison between conversions of cellulose (*X*) and selectivities (*S*) and yields (*Y*) of products obtained after 1 and 5 h of reaction.

Entry	Catalyst	1 h of reaction			5 h of reaction									
		<i>X</i> (%)	<i>S</i> _{sorbitol} (%)	<i>Y</i> _{sorbitol} (%)	<i>X</i> (%)	<i>S</i> _{sorbitol} (%)	<i>Y</i> _{sorbitol} (%)	<i>S</i> _{mannitol} (%)	<i>S</i> _{glucose} (%)	<i>S</i> _{glycerol} (%)	<i>S</i> _{erythritol} (%)	<i>S</i> _{EG} (%)	<i>S</i> _{SPG} (%)	<i>S</i> _{others} (%)
1	Ru/AC	61.1	42.8	26.2	87.8	48.0	42.1	3.4	8.5	6.3	4.7	6.2	7.5	15.4
2	Ni/AC	41.8	15.0	6.3	77.9	8.9	6.9	0.0	10.2	12.9	1.6	0.0	0.0	66.4
3	Ru-Ni/AC	54.1	58.6	31.7	88.3	58.7	51.8	10.8	0.0	5.1	5.6	0.0	0.0	19.8
4	Ru/AC + Ni/AC	59.5	46.1	27.4	88.4	49.0	43.3	6.1	0.0	4.6	3.0	0.0	0.0	37.3
5	Ru-Ni/AC ^a	86.1	86.3	74.3	86.6	80.1	69.4	6.9	0.0	5.9	3.6	0.0	0.0	3.5
6	Ru-Ni/AC ^b	54.2	24.4	13.2	80.2	25.4	20.4	0.0	10.6	4.5	0.3	7.7	14.6	36.9
7	Ru/CNT	52.9	46.9	24.8	83.5	60.9	50.9	2.2	0.0	5.5	8.7	4.9	2.0	15.8
8	Ni/CNT	49.3	13.4	6.6	89.3	8.5	7.6	0.0	9.2	7.0	0.7	5.7	1.4	67.5
9	Ru-Ni/CNT	74.5	55.6	41.4	99.7	61.2	61.0	8.8	7.5	4.1	4.2	4.9	1.3	8.0
10	Ru/CNT + Ni/CNT	38.6	41.5	16.0	100	51.7	51.7	6.0	7.5	4.2	3.3	5.0	1.8	20.5
11	Ru-Ni/CNT ^a	99.3	71.3	70.8	100	64.4	64.4	5.5	0.0	4.5	2.4	4.3	1.1	17.8
12	Ru-Ni/CNT ^b	78.3	47.4	37.1	99.4	63.6	63.2	2.2	7.5	4.4	2.4	4.8	1.5	13.6
13	Ru/CNT_500	51.6	24.6	12.7	96.4	17.9	17.3	1.1	0.0	7.4	8.5	0.0	0.0	65.1
14	Ru-Ni/CNT_500	45.1	53.8	24.3	91.3	53.1	48.5	6.7	0.0	1.1	5.0	0.0	0.0	34.1

^a Cellulose and catalyst were ball-milled together at 20 Hz for 4 h.

^b Besides cellulose, the catalyst was also ball-milled under the same conditions (20 Hz for 4 h).

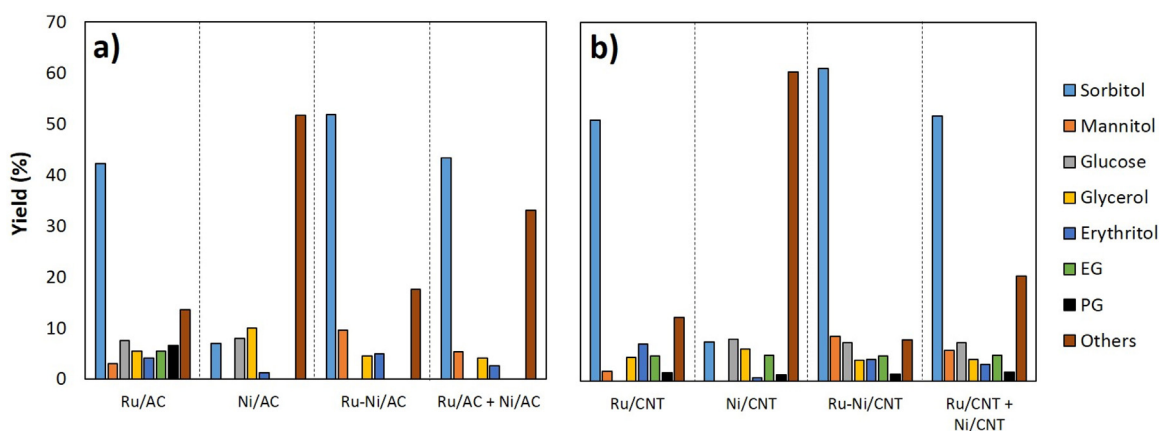


Fig. 6. Effect of Ni on the yield of products after 5 h of reaction using a) activated carbon and b) carbon nanotubes as catalysts supports. Reaction conditions: ball-milled cellulose (0.75 g), catalyst (0.3 g), water (300 mL), 50 bar H₂, 205 °C, 150 rpm.

The effect of the heat treatment and reduction temperatures of Ru-Ni/CNT catalyst was also studied as consequence of using different methods for Ni impregnation. For comparative purposes, this effect was also studied for Ru/CNT catalyst. As depicted in Fig. 7, the yield of sorbitol after 5 h of reaction drastically decreased from 50.9 to 17.3% when using the Ru monometallic catalyst treated and reduced at 500 °C (Ru/CNT_500) in comparison to the Ru/CNT catalyst (treated and reduced at 250 °C, as described in Section 2.2). On the other hand, the yield of non-identified products greatly

increased from 13.2 to 62.8%. The yield of sorbitol after 5 h also decreased, from 61.0 to 48.5%, using Ru-Ni/CNT_500 comparatively to Ru-Ni/CNT, as well as the conversion, whereas the yield of non-identified products largely increased (Fig. 7); this can be related to the fact that the increase of the heat treatment and reduction temperatures promotes the sintering of the metals, that could be easily noticed by the broadening of the particle size distribution of the catalysts prepared at higher temperatures (Figs. 3 and 4). Consequently, the observed increase of metal particle size and decrease

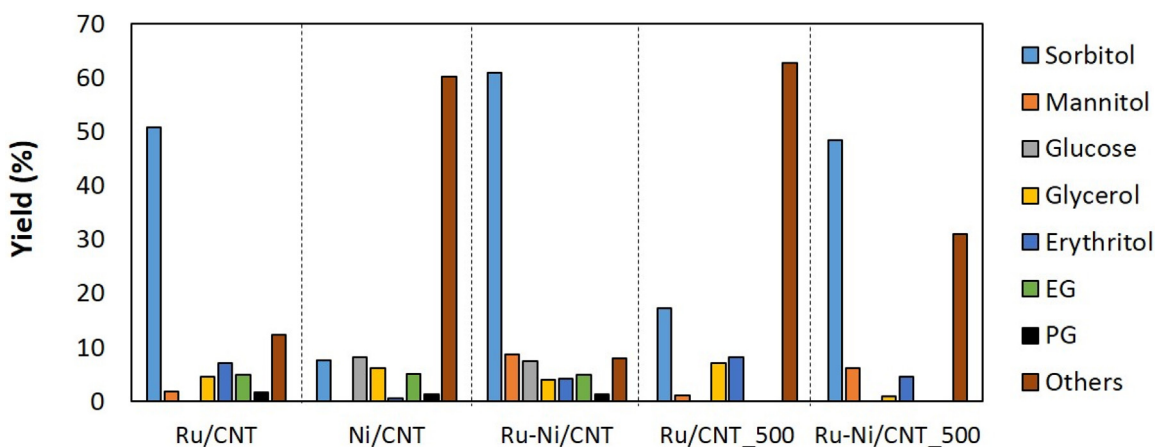


Fig. 7. Effect of the catalyst preparation method on the yield of products after 5 h of reaction. Reaction conditions: ball-milled cellulose (0.75 g), catalyst (0.3 g), water (300 mL), 50 bar H₂, 205 °C, 150 rpm.

in metal dispersion can be prejudicial to the process since Ru atoms are active sites for the direct conversion of cellulose to sorbitol. The distributions of products for Ru/CNT_500 and Ru-Ni/CNT_500 were modified due to the disappearance of some compounds such as EG and PG, as well as glucose in the case of Ru-Ni/CNT_500 (Table 3). Interestingly, despite the conversion of cellulose after 1 h of reaction being significantly higher for Ru-Ni/CNT than Ru-Ni/CNT_500, that difference is softened after 5 h of reaction. On the contrary, the conversion of cellulose achieved after 5 h of reaction was higher when using Ru/CNT_500 instead of Ru/CNT.

As reported by our group in previous works [25,36], the activity and selectivity to sorbitol can be greatly increased if the catalyst is ball-milled together with cellulose (denoted as mix-milling) prior to use in the reaction, which can be related to the good physical contact between the solid substrate and the catalyst. Other works have also reported that this mix-milling can simultaneously amorphize cellulose and facilitate the good solid–solid contact, which results in an increase in the hydrolysis rate relative to the rate of the reaction in which the components (cellulose and catalyst) are individually ball-milled [10,38]. We have previously shown that performing the hydrolytic hydrogenation with the mix-samples (catalyst + cellulose) resulted in a 100% conversion of cellulose in just 1 h of reaction, with 60% selectivity to sorbitol, either using Ru/AC or Ru/CNT as catalyst [36]. Accordingly, in this work a similar study was performed for Ru-Ni/AC and Ru-Ni/CNT. Fig. 8 presents the evolution of cellulose conversion with the reaction time, where a great increase in the initial reaction rate after mix-milling is evident for both Ru-Ni catalysts. This behaviour is comparable with the results previously reported by our group, when using the respective Ru monometallic catalysts [36]. Such increase in the initial reaction rate is not observed when the catalyst and cellulose were separately ball-milled (curves in green in Fig. 8), which allowed concluding that the enhancement of the reaction performance by mix-milling is not due to the catalyst ball-milling but due to the intimate mixing between the two solids (cellulose and catalyst), as mentioned before. Also, thanks to the insoluble properties of both cellulose and catalyst, we believe that the mixed state can continue during the hydrolysis of cellulose. As already reported by Kobayashi et al., the mix-milling as pre-treatment has as main goal the improvement of the contact between the solid catalyst and cellulose, since if we consider that the hydrolysis of cellulose catalysed by a carbon supported metal catalyst occurs at the solid–solid interface, their distance would be a major obstacle in this type of reaction [10]. As so, with the mix-milling, the final conversions of cellulose (86 and 100% for Ru-Ni/AC and Ru-Ni/CNT, respectively) could be achieved after just 30–45 min of reaction. Despite the fact

that the conversion of cellulose after 1 h of reaction was lower using Ru-Ni/AC mix-milled comparatively to Ru-Ni/CNT mix-milled, the selectivity to sorbitol achieved was greater (Table 3).

For both catalysts, the hydrolytic hydrogenation of these mix-milled samples also resulted in a great increase in the yield of sorbitol (Fig. 9). For the Ru-Ni/AC catalyst, the yield of sorbitol attained after 1 h of reaction could be increased from 31.7 to 74.3% by the mix-milling. The Ru-Ni/CNT mix-milled sample also showed an increase in the yield of sorbitol from 41.4 to 70.8% after 1 h. When mix-milled, the Ru-Ni catalysts allowed reaching higher yields of our product of interest and much lower yields of non-identified products, which greatly decreased from 53.8 to 9.0% using Ru-Ni/AC and from 39.3 to 12.7% using Ru-Ni/CNT. This improvement in the yield of sorbitol is not due to the ball-milling of the catalyst, since when the catalysts and cellulose were separately ball-milled, the yield of sorbitol decreased from 31.7 to 13.2% using Ru-Ni/AC and from 41.4 to 37.1% using Ru-Ni/CNT, followed by an increase in the yields of by-products (Fig. 9). To conclude, the major advantage of mix-milling the catalysts and cellulose is to reach yields of sorbitol over 70% in just 1 h of reaction (Table 3 and Fig. 9).

Furthermore, recycling tests of the bimetallic catalysts were performed in order to evaluate the stability. For the conversion of ball-milled cellulose, the Ru-Ni/CNT catalyst was separated from the reaction mixture by filtration, washed with water and dried in an oven overnight. However, in the case of the Ru-Ni/AC catalyst, after filtration from the reaction mixture and drying, the catalyst had to be sieved in order to be separated from the remaining non-converted cellulose, since the conversion in this case was not 100%. Recycling tests were also performed for the conversion of mix-milled cellulose with Ru-Ni/CNT, but could not be performed using mix-milled cellulose and Ru-Ni/AC due to the difficult separation of the catalyst from cellulose after mix-milling and since the conversion achieved was not 100%. The recovered catalysts were then used in successive tests. No significant changes were observed in the yield of sorbitol (Fig. S4), indicating that the bimetallic catalysts can be reused at least up to four cycles, even if mix-milled with cellulose, without metal leaching into solution and without loss in activity and selectivity.

Some works evaluating the effect of bimetallic catalysts on the conversion of cellulose have already been reported in literature [30,31,33,34,39]. Pang et al. developed Ni-based bimetallic catalysts supported on activated carbon and on mesoporous carbon (MC) for the catalytic conversion of cellulose to hexitols [30]. In the conversion of microcrystalline cellulose, this group obtained a selectivity to sorbitol of 41.6% after just 30 min of reaction, with 100% conversion of cellulose, using a 1%Ru-5%Ni/MC catalyst at

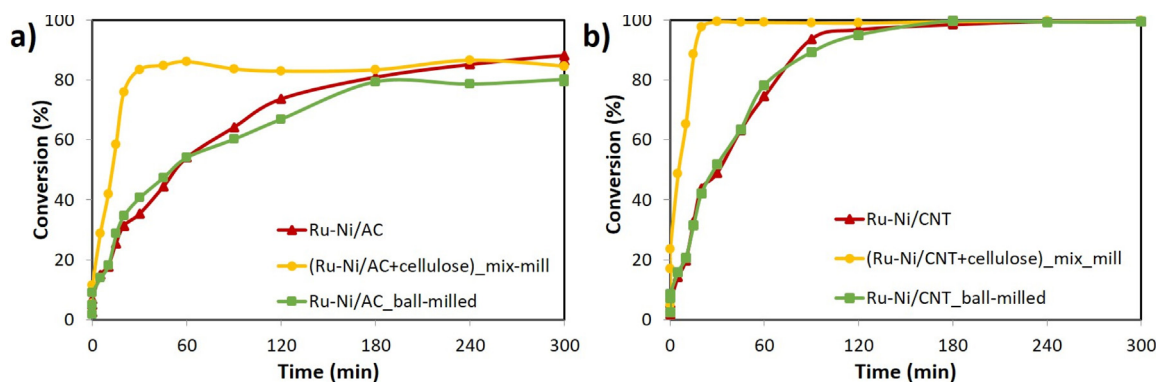


Fig. 8. Evolution of the conversion of cellulose ball-milled together with a) Ru-Ni/AC and b) Ru-Ni/CNT. Reaction conditions: ball-milled cellulose (0.75 g), catalyst (0.3 g), water (300 mL), 50 bar H_2 , 205 °C, 150 rpm.

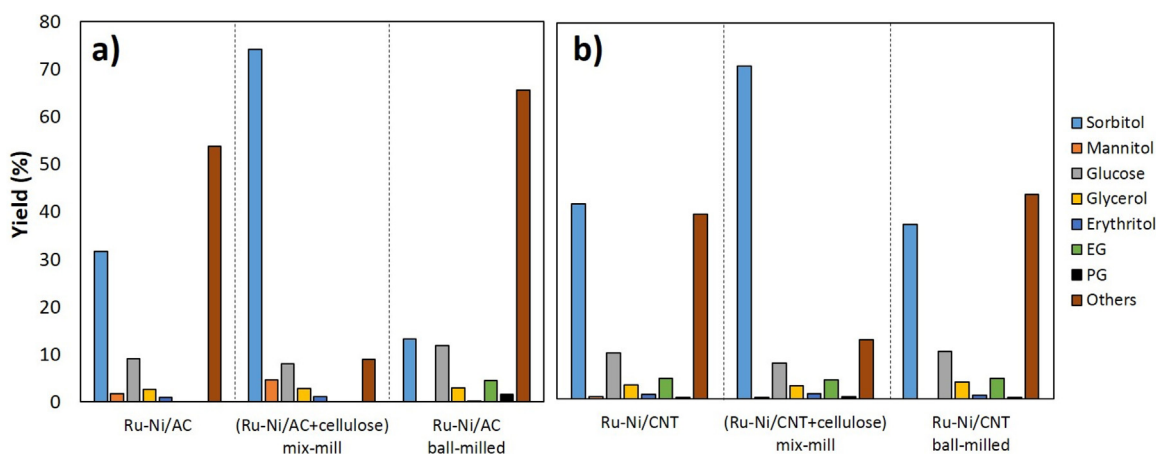


Fig. 9. Effect of ball-milling on the yield of products after 1 h of reaction using a) Ru-Ni/AC and b) Ru-Ni/CNT as catalysts. Reaction conditions: ball-milled cellulose (0.75 g), catalyst (0.3 g), water (300 mL), 50 bar H_2 , 205 °C, 150 rpm.

245 °C and 60 bar of H_2 . We were able to outperform these results in the present work, using less drastic conditions (205 °C and 50 bar H_2) and ball-milling as pre-treatment of cellulose. Although being difficult to properly compare the results obtained in this work to those reported in literature due to the different experimental conditions used, with the combined use of a bimetallic catalyst and its mix-milling with cellulose, to the best of our knowledge, this work reports one of the highest sorbitol yields ever attained using an environmentally friendly one-pot approach for converting cellulose.

4. Conclusions

Ru and Ni mono- and bimetallic catalysts supported on two different carbon materials (activated carbon and carbon nanotubes) were tested in the hydrolytic hydrogenation of cellulose to sorbitol. The Ru mono- and bimetallic catalysts were in general highly efficient, unlike to the Ni monometallic catalysts. In the case of Ru-Ni catalysts, the results show that the presence of Ni improved the catalytic performance of the Ru monometallic catalysts both in terms of activity and selectivity to the product of interest. Yields of sorbitol around 50–60% were achieved after 5 h of reaction when using Ru-Ni/AC and Ru-Ni/CNT as catalysts. The physical mixture of Ru and Ni monometallic catalysts showed no enhancing effect on the sorbitol yield, confirming the synergic effects in Ru-Ni catalysts. Additionally, if the Ru-Ni catalysts were ball-milled together with cellulose, yields of sorbitol over 70% could be reached in just 1 h of reaction. To finish, using higher heat treatment and reduction temperatures

during the catalyst synthesis induced sintering of metal particles, which in turn lowered its activity and selectivity for cellulose direct conversion into sorbitol.

Acknowledgements

This work was financially supported by: project POCI-01-0145-FEDER-006984 – Associate Laboratory LSRE-LCM funded by FEDER funds through COMPETE2020 – Programa Operacional Competitividade e Internacionalização (POCI) – and by national funds through FCT – Fundação para a Ciência e a Tecnologia. J.J. Delgado is grateful to Ramon y Cajal program and the ATOM project from MINECO. L.S. Ribeiro acknowledges her Ph.D. scholarship (SFRH/BD/86580/2012) from FCT.

Appendix A. Supplementary data

Supplementary data associated with this article can be found, in the online version, at <http://dx.doi.org/10.1016/j.apcatb.2017.04.078>.

References

- [1] B.T. Kusema, L. Faba, N. Kumar, P. Mäki-Arvela, E. Díaz, S. Ordóñez, T. Salmi, D.Y. Murzin, Hydrolytic hydrogenation of hemicellulose over metal modified mesoporous catalyst, *Catal. Today* 196 (2012) 26–33.
- [2] A.M. Ruppert, K. Weinberg, R. Palkovits, Hydrogenolysis goes bio: from carbohydrates and sugar alcohols to platform chemicals, *Angew. Chem. Int. Edit.* 51 (2012) 2564–2601.

- [3] P. Yang, H. Kobayashi, A. Fukuoka, Recent developments in the catalytic conversion of cellulose into valuable chemicals, *Chin. J. Catal.* 32 (2011) 716–722.
- [4] A. Romero, E. Alonso, Á. Sastre, A. Nieto-Márquez, Conversion of biomass into sorbitol: cellulose hydrolysis on MCM-48 and d-glucose hydrogenation on Ru/MCM-48, *Micropor. Mesopor. Mater.* 224 (2016) 1–8.
- [5] I. Murillo Leo, J.L.G. López Granados, R. Mariscal, Selective conversion of sorbitol to glycols and stability of nickel–ruthenium supported on calcium hydroxide catalysts, *Appl. Catal. B-Environ.* 185 (2016) 141–149.
- [6] M. Kåldström, N. Kumar, D.Y. Murzin, Valorization of cellulose over metal supported mesoporous materials, *Catal. Today* 167 (2011) 91–95.
- [7] S. Dutta, S. Pal, Promises in direct conversion of cellulose and lignocellulosic biomass to chemicals and fuels: combined solvent–nanocatalysis approach for biorefinery, *Biomass Bioenerg.* 62 (2014) 182–197.
- [8] T. Werpy, G. Petersen, *Top Value-Added Chemicals from Biomass. Volume 1: Results of Screening for Potential Candidates from Sugars and Synthesis Gas* (U.S. Department of Energy, Energy Efficiency and Renewable Energy, Battelle), 2004.
- [9] J. Xi, Y. Zhang, Q. Xia, X. Liu, J. Ren, G. Lu, Y. Wang, Direct conversion of cellulose into sorbitol with high yield by a novel mesoporous niobium phosphate supported Ruthenium bifunctional catalyst, *Appl. Catal. A-Gen.* 459 (2013) 52–58.
- [10] H. Kobayashi, M. Yabushita, T. Komanoya, K. Hara, I. Fujita, A. Fukuoka, High-yielding one-pot synthesis of glucose from cellulose using simple activated carbons and trace hydrochloric acid, *ACS Catal.* 3 (2013) 581–587.
- [11] S. Van de Vyver, L. Peng, J. Geboers, H. Schepers, F. de Clippel, C.J. Gommers, B. Goderis, P.A. Jacobs, B.F. Sels, Sulfonated silica/carbon nanocomposites as novel catalysts for hydrolysis of cellulose to glucose, *Green Chem.* 12 (2010) 1560–1563.
- [12] A. Onda, T. Ochi, K. Yanagisawa, Hydrolysis of cellulose selectively into glucose over sulfonated activated-carbon catalyst under hydrothermal conditions, *Top. Catal.* 52 (2009) 801–807.
- [13] H. Kobayashi, Y. Ito, T. Komanoya, Y. Hosaka, P.L. Dhepe, K. Kasai, K. Hara, A. Fukuoka, Synthesis of sugar alcohols by hydrolytic hydrogenation of cellulose over supported metal catalysts, *Green Chem.* 13 (2011) 326–333.
- [14] X. Guo, X. Wang, J. Guan, X. Chen, Z. Qin, X. Mu, M. Xian, Selective hydrogenation of D-glucose to D-sorbitol over Ru/ZSM-5 catalysts, *Chin. J. Catal.* 35 (2014) 733–740.
- [15] H. Kobayashi, T. Komanoya, S.K. Guha, K. Hara, A. Fukuoka, Conversion of cellulose into renewable chemicals by supported metal catalysis, *Appl. Catal. A-Gen.* 409–410 (2011) 13–20.
- [16] A. Nego, K. Triantafyllidis, V.I. Parvulescu, S.M. Coman, The hydrolytic hydrogenation of cellulose to sorbitol over M (Ru, IrPd,Rh)-BEA-zeolite catalysts, *Catal. Today* 223 (2014) 122–128.
- [17] M. Zheng, J. Pang, A. Wang, T. Zhang, One-pot catalytic conversion of cellulose to ethylene glycol and other chemicals: from fundamental discovery to potential commercialization, *Chin. J. Catal.* 35 (2014) 602–613.
- [18] R. Palkovits, K. Tajvidi, A.M. Ruppert, J. Procelewska, Heteropoly acids as efficient acid catalysts in the one-step conversion of cellulose to sugar alcohols, *Chem. Commun.* 47 (2011) 576–578.
- [19] A. Fukuoka, P. Dhepe, Catalytic conversion of cellulose into sugar alcohols, *Angew. Chem. Int. Edit.* 45 (2006) 5161–5163.
- [20] M. Yabushita, H. Kobayashi, A. Fukuoka, Catalytic transformation of cellulose into platform chemicals, *Appl. Catal. B-Environ.* 145 (2014) 1–9.
- [21] C. Luo, S. Wang, H. Liu, Cellulose conversion into polyols catalysed by reversible formed acids and supported ruthenium clusters in hot water, *Angew. Chem. Int. Edit.* 46 (2007) 7636–7639.
- [22] W. Deng, X. Tan, W. Fang, Q. Zhang, Y. Wang, Conversion of cellulose into sorbitol over carbon nanotube-supported ruthenium catalyst, *Catal. Lett.* 133 (2009) 167–174.
- [23] J. Geboers, S. Van de Vyver, K. Carpentier, K. de Blohouse, P. Jacobs, B. Sels, Efficient catalytic conversion of concentrated cellulose feeds to hexitols with heteropoly acids and Ru on carbon, *Chem. Commun.* 46 (2010) 3577–3579.
- [24] T. Komanoya, H. Kobayashi, K. Hara, W.-J. Chun, A. Fukuoka, Kinetic study of catalytic conversion of cellulose to sugar alcohols under low-pressure hydrogen, *ChemCatChem* 6 (2014) 230–236.
- [25] L.S. Ribeiro, J.J.M. Órfão, M.F.R. Pereira, Enhanced direct production of sorbitol by cellulose ball-milling, *Green Chem.* 17 (2015) 2973–2980.
- [26] G. Liang, L. He, H. Cheng, W. Li, X. Li, C. Zhang, Y. Yu, F. Zhao, The hydrogenation/dehydrogenation activity of supported Ni catalysts and their effect on hexitols selectivity in hydrolytic hydrogenation of cellulose, *J. Catal.* 309 (2014) 468–476.
- [27] L.N. Ding, A.Q. Wang, M.Y. Zheng, T. Zhang, Selective transformation of cellulose into sorbitol by using a bifunctional nickel phosphide catalyst, *ChemSusChem* 3 (2010) 818–821.
- [28] P. Yang, H. Kobayashi, K. Hara, A. Fukuoka, Phase change of nickel phosphide catalysts in the conversion of cellulose into sorbitol, *ChemSusChem* 5 (2012) 920–926.
- [29] S. Van de Vyver, J. Geboers, M. Dusselier, H. Schepers, T. Vosch, L. Zhang, G. Van Tendeloo, P.A. Jacobs, B.F. Sels, Selective bifunctional catalytic conversion of cellulose over reshaped Ni particles at the tip of carbon nanofibers, *ChemSusChem* 3 (2010) 698–701.
- [30] J. Pang, A. Wang, M. Zheng, Y. Zhang, Y. Huang, X. Chen, T. Zhang, Catalytic conversion of cellulose to hexitols with mesoporous carbon supported Ni-based bimetallic catalysts, *Green Chem.* 14 (2012) 614–617.
- [31] M. Sankar, N. Dimitratos, P.J. Miedziak, P.P. Wells, C.J. Kiely, G.J. Hutchings, Designing bimetallic catalysts for a green and sustainable future, *Chem. Soc. Rev.* 41 (2012) 8099–8139.
- [32] Y. Liu, C. Luo, H. Liu, Tungsten trioxide promoted selective conversion of cellulose into propylene glycol and ethylene glycol on a ruthenium catalyst, *Angew. Chemie* 124 (2012) 3303–3307.
- [33] D.M. Alonso, S.G. Wettstein, J.A. Dumesic, Bimetallic catalysts for upgrading of biomass to fuels and chemicals, *Chem. Soc. Rev.* 41 (2012) 7965–8216.
- [34] M.Y. Zheng, A.Q. Wang, N. Ji, J.F. Pang, X.D. Wang, T. Zhang, Transition metal-tungsten bimetallic catalysts for the conversion of cellulose into ethylene glycol, *ChemSusChem* 3 (2010) 63–66.
- [35] S. Bernal, F.J. Botana, J.J. Calvino, C. López-Cartes, J.A. Pérez-Omil, J.M. Rodríguez-Izquierdo, The interpretation of HREM images of supported metal catalysts using image simulation: profile view images, *Ultramicroscopy* 72 (1998) 135–164.
- [36] M. López-Haro, J.J. Delgado, J.M. Cies, E. del Rio, S. Bernal, R. Burch, M.A. Cauqui, S. Trasobares, J.A. Pérez-Omil, P. Bayle-Guillemaud, J.J. Calvino, Bridging the gap between co adsorption studies on gold model surfaces and supported nanoparticles, *Angew Chem Int Edit* 49 (2010) 1981–1985.
- [37] L.S. Ribeiro, Catalytic conversion of lignocellulosic biomass by hydrolytic hydrogenation, in: PhD Thesis, Faculty of Engineering, University of Porto, 2017.
- [38] A. Shrotri, H. Kobayashi, A. Fukuoka, Mechanochemical synthesis of a carboxylated carbon catalyst and its application in cellulose hydrolysis, *ChemCatChem* 8 (2016) 1059–1064.
- [39] T. Deng, H. Liu, Promoting effect of SnOx on selective conversion of cellulose to polyols over bimetallic Pt-SnOx/Al2O3 catalysts, *Green Chem.* 15 (2013) 116–124.